Available online at www.sciencedirect.com
ScienceDirect
International Journal of Heat and Mass Transfer 50 (2007) 4986–4998
International Journal of HEAT and MASS TRANSFER
www.elsevier.com/locate/ijhmt

Conjugate heat transfer in fractal-shaped microchannel network heat sink for integrated microelectronic cooling application

F.J. Hong [a], P. Cheng [a,*], H. Ge [a], Goh Teck Joo [b]

[a] Centre for Microfluidics and Thermal Control, School of Mechanical and Power Engineering, Shanghai Jiao Tong University, 800 Dong Chuan Road, Shanghai 200030, PR China
[b] Intel China Ltd., 999, Ying Lun Road, Pudong, Shanghai 200131, PR China

Received 21 July 2006; received in revised form 16 February 2007
Available online 5 November 2007

Abstract

The hydrodynamic and thermal characteristics of fractal-shaped microchannel network heat sinks are investigated numerically by solving three-dimensional N–S equations and energy equation, taking into consideration the conjugate heat transfer in microchannel walls. It is found that due to the structural limitation of right-angled fractal-shaped microchannel network, hotspots may appear on the bottom wall of the heat sink where the microchannels are sparsely distributed. With slight modifications in the fractal-shaped structure of microchannels network, great improvements on hydrodynamic and thermal performance of heat sink can be achieved. A comparison of the performance of modified fractal-shaped microchannel network heat sink with parallel microchannels heat sink is also conducted numerically based on the same heat sink dimensions. It is found that the modified fractal-shaped microchannel network is much better in terms of thermal resistance and temperature uniformity under the conditions of the same pressure drop or pumping power. Therefore, the modified fractal-shaped microchannel network heat sink appears promising to be used for microelectronic cooling in the future.

1. Introduction

The performance of microelectronic devices has been greatly enhanced owing to the development of the very large-scale integration (VLSI) technology. However, with the increase of circuit density and operating speed, more heat is generated by microelectronic devices. It is anticipated that the next generation of microprocessors and microelectronic components will have to dissipate heat flux in excess of 1000 W/cm^2 [1]. Traditional air cooling [2] is insufficient to dissipate such a high heat flux, and therefore other means of thermal management must be developed for the cooling of microelectronic chips in the future.

Since proposed by Tuckerman and Pease [3], parallel microchannels heat sinks using single-phase water as coolant have emerged as one of the effective and promising cooling techniques for microelectronic cooling. For this reason, many studies have been devoted to fluid flow and heat transfer characteristics of forced convection of water in a single microchannel [4–7]. Recently, some studies [8,9] have also been carried out for a network of parallel microchannels as required in practical applications of electronic cooling. In microchannel heat sinks, a large amount of heat generated by the semiconductor chips is carried out from the package by a relatively small amount of coolant, resulting in a high temperature rise along the microchannels, which causes the non-uniform temperature distribution on the chips. This non-uniformity of temperature is undesirable for several reasons. Firstly, the spatial temperature gradient may adversely affect the performance of electronic devices. Secondly, large temperature non-uniformity can produce potentially destructive thermal stresses in elements and packages due to the differences in the thermal expansion coefficient, which poses potential reliability concerns to the devices. The bulk temperature rise along the

* Corresponding author. Tel./fax: +86 21 6293 3107.
E-mail address: pingcheng@sjtu.edu.cn (P. Cheng).

0017-9310/$ - see front matter © 2007 Elsevier Ltd. All rights reserved.
doi:10.1016/j.ijheatmasstransfer.2007.09.006

Nomenclature

c_p	specific heat capacity
D	hydraulic diameter
h	convective heat transfer coefficient
H	channel depth
k	thermal conductivity
L	channel length
m	number of branch level
$\dot{m}$	mass flow rate
p	pressure
q	heat flux
Q	heat transfer rate
T	temperature
$\boldsymbol{V}$	velocity vector
W	channel width
x, y, z	coordinates

Greek symbols

α	thermal diffusivity
β	channel diameter ratio
γ	channel length ratio
ψ	thermal resistance
ρ	density
μ	dynamic viscosity
$\boldsymbol{\tau}$	viscous stress tensor
ξ	local coordinate
υ	kinetic viscosity

Subscripts

c	coolant
in	inlet
k	branch level
max	maximum
min	minimum
0	branch zero
s	heat sink
w	wall

channels can be reduced by increasing the mass flow rate of the coolant, which however causes a larger pressure drop, thereby consuming more pumping power, generating more noise and requiring bulkier packaging to resist higher pressure. Thus, there exists a need to develop new type of microchannel heat sinks that not only have lower thermal resistance but also smaller pressure drop and better temperature uniformity.

Bejan [10] firstly proposed heat conduction paths using tree-shaped network base on the constructal theory for the cooling of heat generating volume. Later, Bejan and Errera [11] developed a tree-shaped parallel-channel network for electronic cooling based on the same constructal theory. These tree-shaped channel networks proposed by Bejan and co-workers based on the constructal theory are non-fractal. Inspired by the fractal pattern of mammalian circulatory and respiratory systems, Pence [12] as well as Chen and Cheng [13] proposed fractal-shaped microchannel networks for the convective cooling of microelectronic components with circular and rectangular geometric shapes. Assuming a thermally and hydrodynamically fully-developed flow and neglecting the conjugate heat transfer in the channel walls, heat transfer and pressure drop characteristics of fractal-shaped network were obtained analytically in the previous work [12,13]. It was found that under the condition of the same convective heat transfer area, the fractal-shaped microchannel network has much higher heat transfer rate and smaller pressure drop than parallel microchannels. Subsequently, Senn and Poulikakos [14] performed a three-dimensional numerical simulation of forced convection in fractal-shaped channel network for thermal management in polymer electrolyte fuel cell. The conjugate heat transfer in the wall was not considered in their analysis but a constant heat flux boundary condition was imposed on the channel walls. A comparison of a fractal-shaped channel network with a serpentine channel was made under the condition of the same convective heat transfer area. Their numerical results indicated that a fractal-shaped microchannel network has a smaller pressure drop, a larger heat transfer rate, and a more uniform temperature distribution than a serpentine channel.

It should be noted that the heating source is often at the bottom of the heat sink (the top of chips) in most of electronic cooling applications. Therefore, the assumptions of uniform heating generating volume [10,11], or constant channel wall heat flux [12,14], or constant temperature difference between the wall and the coolant [13] are not realistic. In addition, a comparison of fractal-shaped microchannel network with parallel microchannels based on the same heat sink dimensions is more practical than that based on the same convective heat transfer area as adopted in previous studies [12–14]. Furthermore, since conjugate heat transfer has been found to have a significant effect in silicon microchannels [15], any calculation of heat transfer characteristics in the microchannel network without considering the conjugate heat transfer in the wall will not be accurate.

Recently, Alharbi and Pence [16] compared the performance of a fractal-shaped microchannel network in a circular heat sink with that of a parallel microchannel using 3-D numerical simulation. A fractal-shaped microchannel network with four branch levels was adopted, and the comparison with parallel microchannels was based on the assumption of same heat sink surface area. They found that the pressure drop of a fractal-shaped microchannel

network with four branch levels was larger than that of parallel microchannels while the thermal resistance was very close. It should be noted that channel density of a fractal-shaped network with four branch levels is too sparse for practical applications of electronic cooling. Furthermore, a comparison of a circular heat sink with that of rectangular heat sink is not straightforward because the channel length of parallel microchannels and the centre to centre distance of the parallel microchannels have to be determined in an arbitrary manner. Alharbi and Pence [16] used the sum of the length of all branch channels in fractal-shaped channel network as the length of parallel microchannels and *assumed* the centre to centre distance of the parallel microchannels to be *double* the channel width. This may be one of the reasons why their numerical results indicated no obvious advantage of fractal-shaped channel network.

In this paper, a numerical study on the hydrodynamic and thermal characteristics of a right-angled fractal-shaped microchannel network heat sink with application to integrated microelectronic cooling is conducted from both fundamental and application points of the view. The right-angled (with T-shape junctions) fractal-shaped microchannel network is different from those with less than right-angled fractal-shaped microchannel network in a previous study [16], with the former more suitable for practical applications of electronic chips which are of rectangular shape. A construction method of fractal-shaped microchannel network, which is suitable for any width to length ratio of a rectangular heat sink, is proposed in this paper. A fractal-shaped microchannel network with six branch levels for a square heat sink with the base dimension of 12 mm × 12 mm × 0.5 mm is constructed. Numerical computations were carried out by solving three-dimensional N–S equations and the energy equation, taking into consideration the conjugate heat transfer in the microchannels walls. The thermal and pressure drop characteristics of the fractal-shaped microchannel network are analyzed in details, and locations of hotspots in the right-angled fractal-shaped microchannel network are identified. Accordingly, some structural modifications of the fractal-shaped microchannel network are made, and great improvements of heat sink performance are achieved. It is found that the modified fractal-shaped microchannel network is much better than the parallel microchannels in terms of thermal resistance and temperature uniformity under the condition of the same pressure drop or pumping power.

2. Generation of fractal-shaped microchannel network

The right-angled fractal-shaped microchannel network as shown in Fig. 1 for cooling of electronic chips is considered in the present study. The microchannel network is to be fabricated in a silicon wafer using the deep reactive ion etch (DRIE) of MEMS technology. Therefore, a rectangular cross-section with uniform channel depth is assumed for all of channel branches. For a fixed channel depth, the following independent parameters should be given to fix the design: the hydraulic diameter and the length of inlet plenum, i.e., the hydraulic diameter d_0 and the channel length L_0 of the branch zero, the ratio of hydraulic diameters $\beta = d_{k+1}/d_k$ between two consecutive branch levels and its corresponding length ratio $\gamma = L_{k+1}/L_k$, the number of branches m.

For a T-shaped junction with fixed total tube volume, according to Murray's law [17], the minimization of flow resistance yields the optimal diameter ratio $\beta = d_{k+1}/d_k = 2^{-1/3}$, which is independent of the length ratio $\gamma = L_{k+1}/L_k$ and geometry. With the space allocated further fixed, i.e., $2L_{k+1}L_k = \text{const.}$, the minimization of flow resistance [18] gives the optimal length ratio $\gamma = L_{k+1}/L_k = 2^{-1/3}$. However, to avoid the overlapping of the channel for a right-angled plane, considering the geometric constraint and neglecting channel width, it requires that

$$\sum_{i=1}^{m/2} L_{2i} \leqslant L_0 \tag{1}$$

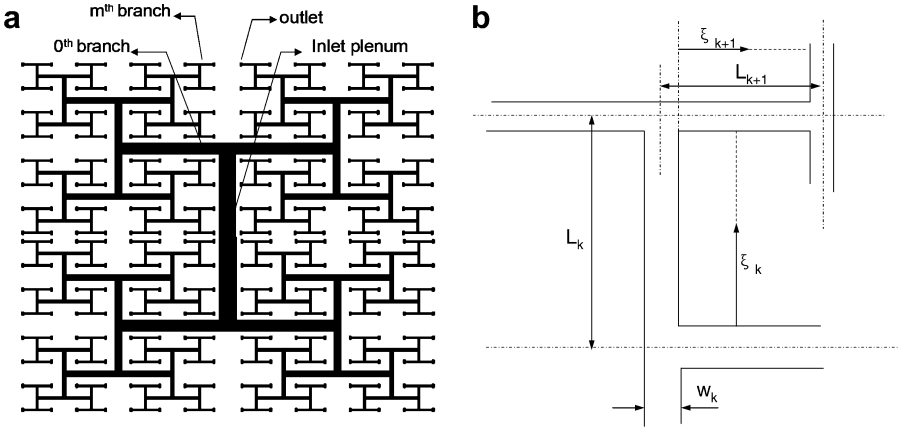

Fig. 1. The schematic of fractal-shaped microchannel network: (a) the structure of the whole microchannel network; (b) the dimensions of the channels: ξ is the local coordinate for the branches, indicating the distance from *the* kth bifurcation.

where m is the branch level. If the optimal channel length ratio is adopted, substituting $L_{k+1}/L_k = 2^{-1/3}$ into Eq. (1) gives

$$\sum_{i=1}^{m/2} 2^{\frac{-2i}{3}} \leqslant 1 \tag{2}$$

Therefore m must be less than 4 to satisfy Eq. (2). However, the channel density of the channel network with four branch levels ($m = 4$) is too sparse in practical applications of microelectronic cooling. In order to construct the fractal-shaped microchannel network with any branch level m and at the same time to avoid the channel overlapping, the length ratio γ should satisfy the following geometric relation,

$$\gamma^2(1 + \gamma^2 + \cdots + \gamma^{m-2}) \leqslant 1 \tag{3}$$

That is

$$\gamma^2 \frac{1-\gamma^m}{1-\gamma^2} \leqslant 1 \tag{4}$$

Obliviously, Eq. (4) is always valid when $\gamma \leqslant 2^{-1/2}$. Actually, the length ratio of $\gamma = 2^{-1/2}$ was also used in the studies of Senn and Poulikakos [13] and Pence [12] to construct the fractal-shaped microchannel network. A practical concern when adopting $\gamma = L_{k+1}/L_k$ for the construction of the fractal-shaped microchannel network is that the ratio of width to length of the heat sink embedded with this network is also fixed and equals to γ, if margins between the channels and the heat sink boundary can be neglected. This will severely limit its application to microelectronic chips with a specific length to width ratio, but is not applicable to chips with any other length to width ratio.

Based on the aforementioned considerations, the following method is proposed to construct the fractal-shaped microchannel network, i.e., the hydraulic diameters ratio of the channels follows the optimal ratio, $d_{k+1}/d_k = 2^{-1/3}$, while the channel length ratio is changed to

$$\begin{aligned} L_k/L_{k+2} &= \gamma_1 \quad (k = 0, 2, 4, \ldots) \\ L_k/L_{k+2} &= \gamma_2 \quad (k = 1, 3, 5, \ldots) \end{aligned} \tag{5}$$

where the values of γ_1 and γ_2 are dependent on the branch level m and are chosen in such a way that it will not lead to the overlapping of the channels, while keeping appropriate margins between the channels, which is determined by the limit of MEMS technology and considering the integrity of the structure. This modification in the construction of channel network will enable its application to a heat sink with any width to length ratio.

3. Heat sink with a single-layered fractal-shaped microchannel network

A double-layered fractal-shaped microchannel network with the highest branch channels connected to each other for forced convection cooling of *rectangular* microelectronic chips was first proposed by Chen and Cheng [13], who performed an analysis on heat transfer and pressure drop of such a microchannel network. A double layered microchannel network was subsequently adopted by Senn and Poulikakos [14] in a numerical study of the cooling of a micro fuel cell. An additional thermal insulation layer was added in their heat sink prototype to separate two layers of microchannel network, where the first layer with lower coolant temperature was for the cooling of the anode and the second layer with higher temperature was for the cathode side of the fuel cell. In this study, we proposed a single-layered structure for microelectronic cooling. This is because the second layer consumes the same pressure head to drive the fluid flow, but it has much lower cooling capability as the coolant has been heated to a relatively high temperature after it flows through the first layer. Therefore, the second layer is not necessary from the energy efficiency point of the view.

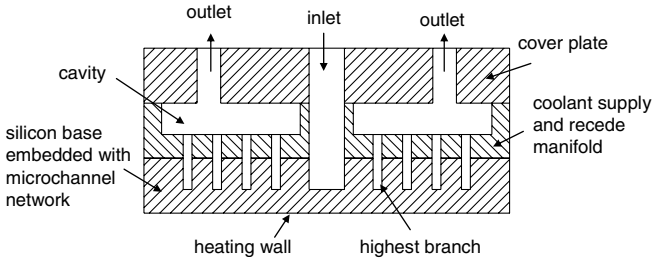

Fig. 2. The schematic of heat sink prototype with single-layered fractal-shaped microchannel.

To circulate the coolant in a single-layered structure, a heat sink prototype as shown in Fig. 2 is designed. The heat sink consists of three components: a silicon wafer embedded with the fractal-shaped microchannel network, a coolant manifold made of thermal insulation material (i.e., Pyrex glass) bonded to silicon wafer to enclose the channels and form the inlet and outlets of the fractal-shaped microchannel, as well as a cover plate bonded with the coolant manifold to form a cavity for collecting the coolant from the highest branches of the fractal-shaped microchannel. The coolant is supplied to silicon base layer through the cover layer and the coolant manifold layer. After it flows through all levels of the branches of the fractal-shaped microchannel network to the highest branch, it is collected in the cavity of the manifold, and through which it finally flows out of the heat sink.

4. Numerical model and scheme

Consider the fractal-shaped microchannel network in a square heat sink as shown in Fig. 2. In order to simplify the numerical simulation, only silicon channel network plate is included in the computational domain by neglecting the heat transfer between the coolant manifold and the silicon base since the manifold is made of thermal insulation material. Furthermore, because of the geometric symmetry, only 1/4 of the silicon base (upper left) as drawn in Fig. 3 is considered to save computational costs.

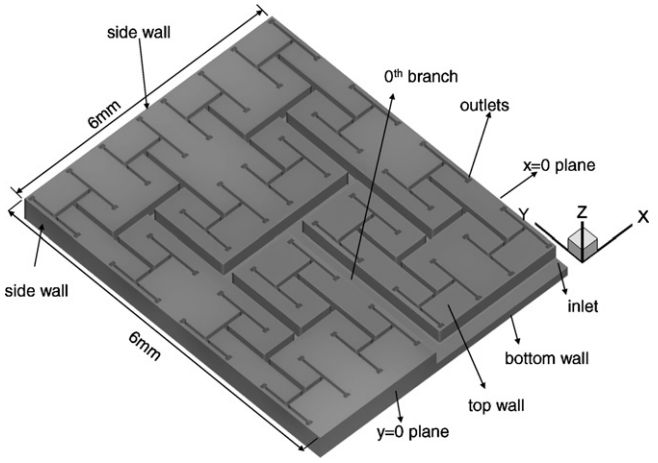

Fig. 3. Three dimensional schematic of computational domain for 1/4 fractal-shaped microchannel network heat sink (symmetric with $x = 0$ and $y = 0$ planes).

The silicon base layer of the heat sink under consideration in this study is 12 mm in width, 12 mm in length and 0.5 mm in thickness. The channel length ratios of $\gamma_1 = 0.5322$ and $\gamma_2 = 0.5343$ are adopted in the construction of microchannel network. The detailed channel size for each branch is summarized in Table 1. DI water is used as the coolant in the present study. Consider the computational domain as shown in Fig. 3, the mathematical formulation is based on the following assumptions:

1. The hydraulic diameter of microchannels under consideration ranges from about 0.04 mm to 0.5 mm, which yields a typical Knudsen number for water between 7.5×10^{-7} and 1.0×10^{-5}. Hence, the conservation equations based on the continuum model (i.e., Navier–Stokes equations) and the non-slip boundary condition on walls are applicable.
2. The transport processes are considered to be at steady state and the fluid flow is incompressible and laminar.
3. Thermal radiation and convection heat transfer to the environment are neglected.
4. The viscous dissipation effect is neglected as Brinkman constant for the present cases is far less than unity.
5. Gravity effects are negligible in momentum equations in fluid flow in microchannels.

Table 1
Channel dimensions for the fractal-shaped microchannel network

k	H_k (mm)	W_k (mm)	d_k (mm)	L_k (mm)	L_k/d_k
Inlet plenum	0.300	0.500	0.378	3.000	7.9
0	0.300	0.300	0.300	2.875	9.6
1	0.300	0.197	0.238	1.596	6.7
2	0.300	0.138	0.189	1.536	8.1
3	0.300	0.100	0.150	0.8497	5.7
4	0.300	0.074	0.119	0.8207	6.9
5	0.300	0.056	0.095	0.4522	4.8
6	0.300	0.043	0.075	0.4385	5.8

6. Thermophysical properties of water and silicon wafer are temperature dependent, as summarized in Table 2.

Under the above assumptions, the conservation equations of mass, momentum and energy can be written for the fluid and conservation of energy for the solid respectively as follows:

Conservation of mass

$$\nabla \cdot \mathbf{V} = 0 \tag{5}$$

Conservation of momentum

$$\nabla \cdot (\mathbf{V}\mathbf{V}) = -\frac{1}{\rho}\nabla p + \frac{1}{\rho}\nabla \cdot \boldsymbol{\tau} \tag{6}$$

where $\boldsymbol{\tau} = 2\mu\left(\frac{1}{2}\left[(\nabla \mathbf{V}) + (\nabla \mathbf{V})^T\right]\right)$ is the stress vector.

Conservation of energy for fluid

$$\nabla \cdot (c_p T \mathbf{V}) - \nabla \cdot (k \nabla T) = 0 \tag{7}$$

Conservation of energy in the walls

$$\nabla \cdot (k \nabla T) = 0 \tag{8}$$

Boundary conditions are needed to close the mathematical formulation. A uniform heat flux q is imposed at the bottom wall of heat sink, while all other external walls are taken to be perfectly thermally insulated with no radiation and convective heat transfer to the environment. Symmetric boundary conditions are applied to the planes at $x = 0$ and $y = 0$, which are the symmetric planes of the heat sink. The velocity (or mass flow rate) and temperature of the fluid entering the inlets of the heat sink are specified, while a constant pressure boundary condition is applied at the outlets. The continuity of temperature and heat flux is used as the conjugate boundary condition to couple the energy equations for the fluid and in the walls.

Eqs. (5)–(8) along with the above described boundary conditions were solved numerically using a finite-volume CFD solver (FLUENT). Structural grids were used for fluid flow in the channel, while non-structural grids were adopted in the walls. Convergence criterion for mass, velocity and energy were 1×10^{-4}, 1×10^{-4} and 1×10^{-7}, respectively. The pressure–velocity coupling was accomplished using the SIMPLE method. The grids near the solid/liquid interface were specially refined (with minimum grid size of 0.005 mm) to resolve viscous shear layer and to capture the conjugate boundary conditions correctly. A careful grid-independent study was performed in order to produce grid-independent results. Additionally, the total energy conservation was examined through comparing the input heat for the system from the bottom wall of heat sink and the increase of coolant internal energy, which was calculated as the difference of the total coolant internal energy at the inlet and the outlets. For all of the cases computed in this study, the relative error was controlled within 0.05%. The numerical simulation was carried out for the cases without considering conjugate heat transfer, and the results were verified by comparing with the results by Senn and Poulikakos [14].

Table 2
Thermophysical properties of DI water and silicon

		DI water [19][a]	Silicon [20,21][a]
μ	Pa s	$0.0194 - 1.065\,\mathrm{e}{-4} \times T + 1.489\,\mathrm{e}{-7} \times T^2$	
k	W/m K	$-0.829 + 0.0079 \times T - 1.04\,\mathrm{e}{-5} \times T^2$	$290 - 0.4 \times T$
c_p	J/kg K	$5348 - 7.42 \times T + 1.17\,\mathrm{e}{-2} \times T^2$	$390 + 0.9 \times T$
ρ	kg/m^3	998.2	2330

[a] Regressed according to the data from the references for the temperature range of 283–373 K (the unit of temperature is Kelvin).

5. Hydrodynamic characteristics of fractal-shaped channel network

To study the hydrodynamic characteristics of the fractal-shaped microchannel network, a numerical investigation of such a network with the geometric size listed in Table 1 was first conducted without considering heat transfer. The material properties of the DI water at 300 K were used and determined according to the correlation equations listed in Table 2.

The existence of T-shaped bifurcations is one of the main characteristics of the right-angled fractal-shaped microchannel network. To illustrate the effect of bifurcation on fluid flow, the velocity vectors of the span-wise (z-direction) and transverse (y-direction) components at several cross-sections of the branch $k = 1$ for the case of mass flow rate $\dot{m} = 0.0018$ kg/s, corresponding to Reynolds number at inlet plenum of about 2200, is shown in Fig. 4. In Fig. 4, ξ_k is the local coordinate denoting the distance from the kth bifurcation. It can be seen that as the flow passes through the bifurcation, the secondary flow patterns, which bring the fluid from outer wall towards inner wall, initiate at the inlet of the branch ($\xi_k = 0$) and diminish gradually with the increasing distance from the bifurcation. The swirl patterns also appear at the locations close to the top and bottom walls at $\xi_k = 0$, and gradually move towards the centre to converge with the increasing of ξ_k. These kinds of flow patterns can enhance the local heat transfer by mixing the cooler water at the centre of the channel with the hotter fluid close to the channel wall. However, it should be noted that the secondary flow pattern will also consume additional pressure head as will be discussed later.

The total pressure drop versus mass flow rate is one of the most important information for the design of microelectronic cooling system. Such information for the fractal-shaped microchannel network is presented in Fig. 5. The pressure drop here is defined as the difference of the average static pressure of the inlet and the outlets. Fig. 5 reveals that the pressure drop variation is non-linear with its gradient increasing with mass flow rate. This is different from parallel microchannels whose pressure drop variation is almost linear with respect to mass flow rate according to the classical theory of a hydrodynamically fully developed laminar flow, which will also be confirmed numerically later in this paper. The non-linear relationship of pressure drop and mass flow rate can be attributed to the bifurcations and the developing of fluid flow at each branch of the fractal-shaped microchannel network. In the fractal-shaped microchannel network, the flow is bifurcated and the secondary flow is initiated at bifurcations, which then decays as it passes along the channel, such that the flow tends to develop again before reaching the next bifurcation. The length of developing segment in a pipe with uniform inlet velocity can be estimated from the classical theory as $l = 0.065Re\,d$ [22]. For the present case, the ratio of channel length to hydraulic diameter L_k/d_k is in the range of 4.8–9.6 as tabulated in Table 1. It can be estimated that

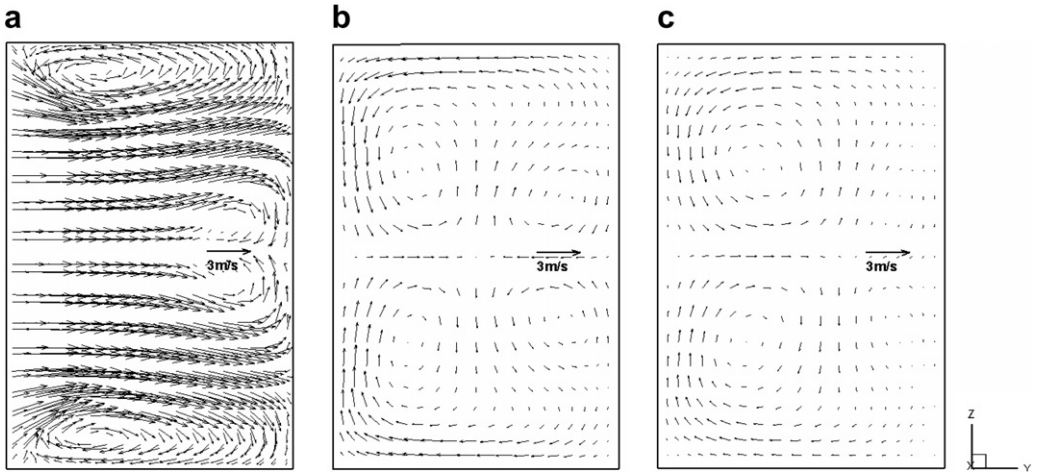

Fig. 4. The secondly flow pattern at cross-sections of channels at branch level $k = 1$: (a) $\xi_k/\xi_{k,\max} = 0$; (b) $\xi_k/\xi_{k,\max} = 0.25$; (c) $\xi_k/\xi_{k,\max} = 0.5$.

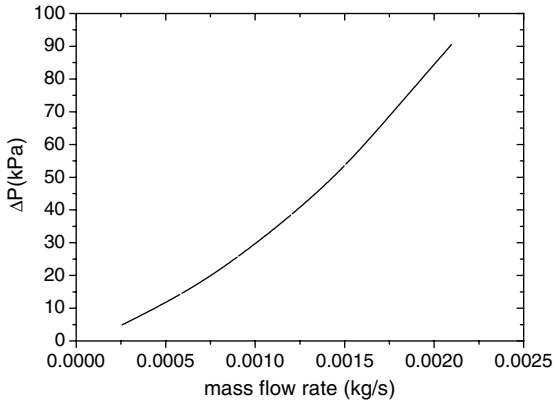

Fig. 5. The pressure drop of the fractal-shaped microchannel network as a function of mass flow rate.

in the range of the mass flow rates in Fig. 5, the calculated lengths of developing segment for low level branches are at the same magnitude with or larger than the branch channel length. Due to the disturbance effect of bifurcations, the flow inlet velocity of the each branch is not uniform, so the actual length of developing segment should be larger than the calculated values. This implies that the fluid flow in the most part of fractal-shaped microchannel network is not hydrodynamically fully developed as had been assumed in the previous analytical studies [12,13]. Moreover, the effect of bifurcation on pressure drop will become more obvious with the increase of flow rate. A more detailed analysis of bifurcation effect and the developing of fluid flow in the fractal-shaped microchannel network can be found elsewhere [14].

6. Thermal characteristics of fractal-shaped channel network heat sink

In this section, numerical results on heat transfer and temperature distribution characteristics of the fractal-shaped microchannel network in a square heat sink are discussed based on a detailed analysis of a baseline case. The heat sink has a base dimension of 12 mm × 12 mm × 0.5 mm, embedded with the fractal-shaped microchannel network whose channel size is summarized in Table 1. The computational conditions for this square heat sink are: the DI water inlet temperature, $T_{c,in} = 300$ K, mass flow rate, $\dot{m} = 0.0018$ kg/s and heat flux, $q = 100$ W/cm^2.

Fig. 6 shows the temperature distribution at the bottom wall of heat sink. Due to the geometric symmetry of the heat sink, only 1/4 of the area is shown. The fractal-shaped microchannel network pattern is also projected onto the surface of the heat sink bottom wall in order to facilitate the analysis. It can be seen from Fig. 6 that the temperature distribution on the base materials beneath the first four branches (inlet plenum, 0th, 1st, and 2nd branch) is much lower than those areas near the heat sink boundaries, where hotspots of the heat sink are formed. This kind of temperature distribution is in fact resulted from the special

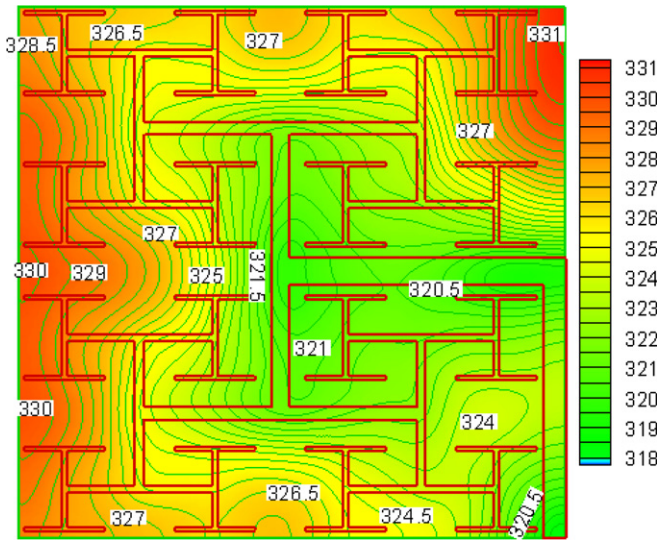

Fig. 6. The temperature distribution at the heating surface (Due to the geometric symmetry, only 1/4 of the area is drawn; the fractal-shaped microchannel network pattern is also projected to the surface.).

structure of the fractal-shaped microchannel network, the conjugate heat transfer in channel walls, as well as heat conduction in the base material as will be explained in details later in this paper.

In a fractal-shaped microchannel network, the fluid flow bifurcates from k branches into $k+1$ branch one by one, and it is being heated gradually along the flow path. So when the coolant arrives at the highest branches, it has already been heated to a relatively high temperature. As a result, the cooling capability of the coolant decreases from k branches to $k+1$ branch. Since the coolant temperature is lower at the first four branches, the cooling capability of the coolant is larger, and consequently the wall temperature beneath them is lower.

The formation of hotspots near the heat sink boundary as shown in Fig. 6 is mainly due to two reasons. Firstly, the cooling capability of the coolant is the lowest at the highest branches. Secondly, the channel density at the highest branches is relatively low. As can be seen from Fig. 6, large blank areas uncovered by channels are around the highest branches areas, although these blank areas are still under heating from the bottom wall of the heat sink because of a uniform heat flux is assumed in this study. This means that the convective heat transfer area of the highest branch (the interface area of channel and base material) for the same amount of heating area is the least near the highest branches of the fractal fractal-shaped microchannel. Although, according to the classical theory, convective heat transfer coefficient of kth branch h_k in the thermally fully developed region scales with $h_k \propto 1/d_k$, which implies that h_k increases from k branch to $k+1$ branch in the fractal-shaped microchannel network, it cannot compensate the effect of the reduction of cooling capability of the coolant and the decrease of convective heat transfer area; therefore, the wall temperature near the highest branches is the

highest according to the Newton's cooling law. Although the assumption of thermally fully developed flow may not be appropriate for the present cases, considering the secondary flow caused by the bifurcations and the small ratio of channel length to hydraulic diameter, the convective heat transfer coefficient is still increasing from k branch to $k+1$ branch according to the study by Senn and Poulikakos [14].

As shown in Fig. 6, the wall temperature beneath different highest branches is not the same, with the temperature close to the first four branches being lower. This is because the base material beneath the first four branches has a lower temperature, which in turn can absorb the heat from its neighborhood through heat conduction in the base material, leading to the gradual increase of the temperature with increasing distance from the first four branches. It should be mentioned that the numerical result without considering conjugate heat transfer and assuming a constant wall heat flux in a previous study [14] predicted no hotspots at the highest branches. This conclusion is contradictory from the present study, indicating the critical role of conjugate heat transfer in a heat sink study.

7. Modification of fractal-shaped microchannel network

To judge the performance of a heat sink for electronic cooling, at least three parameters: pressure drop, thermal resistance and temperature uniformity, should be considered. The pressure drop of the heat sink is the total pressure head required to drive a certain amount of coolant through the heat sink. As pointed out in the introduction section of the paper, a heat sink with high pressure drop will cause noise and require a bulkier packaging. The second parameter to be considered is the thermal resistance of a heat sink, which is defined as:

$$\psi_s = \frac{T_{s,\max} - T_{c,in}}{Q} \tag{9}$$

where $T_{s,max}$ is the maximum temperature at the heat sink bottom wall, $T_{c,in}$ the coolant inlet temperature, and Q the dissipated heat rate. Since the thermal solution for electronic cooling must ensure the temperature at the hottest location of the chip below a specified value, the thermal resistance of heat sink actually determines the maximum heat flux allowed to be dissipated by the heat sink. Besides pressure drop and thermal resistance, another important factor needs to consider is the temperature uniformity. The temperature uniformity as mentioned in the introduction section of this paper affects the stability, reliability and performance of the chips and is often quantified by

$$\Delta T_s = T_{s,\max} - T_{s,\min} \tag{10}$$

where $T_{s,min}$ is the minimum temperature at the heat sink bottom wall. According to Eqs. (9) and (10), the hotspots in Fig. 6 (which corresponds to $T_{s,max}$) will not only deteriorate the thermal resistance but also the temperature uniformity of the heat sink. Therefore, any modifications in microchannel distribution for reducing the temperature at hotspots are desirable to improve the heat sink thermal performance.

As discussed above, in the construction of a fractal-shaped microchannel network, the optimization principle of channel diameter ratio based on Murray's law [17] was utilized. However, it should be noted that the precondition of optimization was based on a fixed total channel volume, and the optimization was for flow resistance but not for heat transfer. For application in microelectronic cooling, both the fluid flow and heat transfer aspects of the channel structure should be considered simultaneously. Moreover, the geometric constraint condition for the practical application is normally the heat sink dimension but not the channel volume. Therefore, it is necessary to reexamine the construction principles of the fractal-shaped channel network for microelectronic cooling applications.

By analyzing the pressure drop composition of the fractal-shaped microchannel network, it is found that the pressure drop is mainly from the first four branches (inlet plenum, 0th, 1st and 2nd branch). Considering the baseline case ($T_{c,in} = 300$ K, $\dot{m} = 0.0018$ kg/s, $q = 100$ W/cm^2), the total pressure drop of the channel network is 62.7 kPa, while the pressure drop of the inlet plenum, 0th branch, 1st branch and 2nd branch is 16.2 kPa, 17.1 kPa, 7.4 kPa and 4.4 kPa, respectively. This indicates that about 72% of pressure head is consumed in the first four branches to drive the fluid flow. At the same time, the wall temperature beneath the first four branches (as shown in Fig. 6) is much lower than the rest of the heat sink. Since the thermal performance of the heat sink is mainly limited by the highest temperature of the heat sink according to Eqs. (9) and (10), the low temperature on the base material beneath the first four branches is not beneficial to the reduction of the thermal resistance. On the contrary, it increases the temperature non-uniformity. Considering the pressure drop as the cost and the thermal performance as the benefit, the large pressure drop in the first four branches is some kind of waste. According to the classical theory of forced convection in channels, the heat transfer coefficient $h \propto 1/d$ and the pressure drop $\Delta P \propto 1/d^4$ for a given mass flow rate. This observation reveals that pressure drop can be reduced considerably by enlarging the channel size of the first four branches, while keeping the temperature at the bottom wall lower than that of hotspots, as the heat transfer coefficient decreases in a much slower rate than that of pressure drop with the increasing of channel diameter. An additional benefit of this modification is the decrease of temperature difference between the hotspots and the low temperature areas, thereby improving the temperature uniformity of the heat sink. The corresponding modification of the channel network is presented in Fig. 7b.

To reduce the thermal resistance of a heat sink, the temperature at hotspots has to be lowered. Two approaches are available to achieve this goal according to the Newton's cooling law: one is to increase the convective heat transfer area and the other is to increase the convective heat

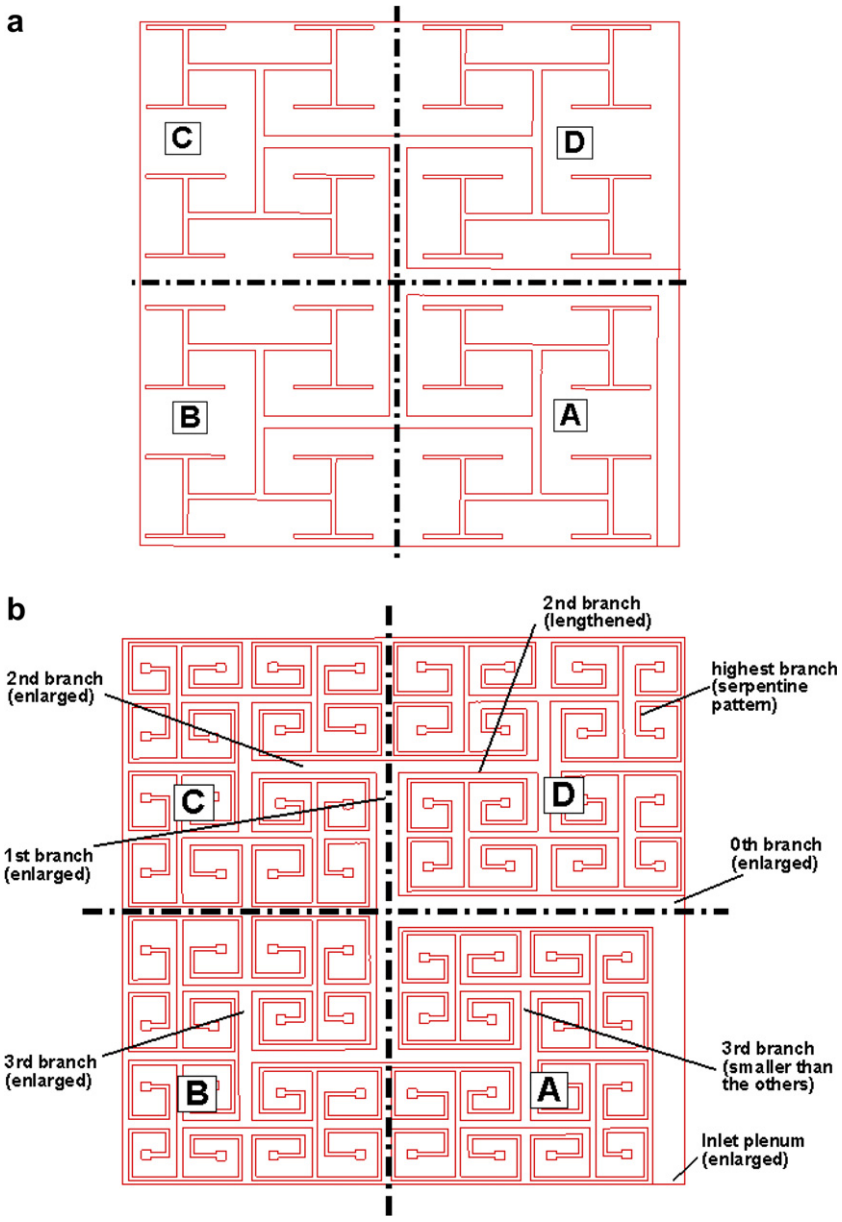

Fig. 7. Fractal-shaped microchannel network structure (drawn to scale): (a) the standard fractal-shaped microchannel network; (b) the modified fractal-shaped microchannel.

transfer coefficient at the highest branch where hotspots appear. A simple way to increase convective heat transfer coefficient is by reducing the hydraulic diameter of channel. However, the pressure drop will increase at a faster rate as discussed before since it is proportional to the fourth power of the reciprocal of channel's hydraulic diameter, in comparison with the first power of the heat transfer coefficient with the reciprocal of channel's hydraulic diameter. So, the method of increasing heat transfer coefficient by decreasing channel's diameter is not economical. The heat transfer area can also be increased by lengthening the channel. Although it will also increase the pressure drop, because the pressure drop is proportional to the first power of channel length, the cost to pay is relatively smaller. Therefore, as shown in Fig. 7b, a serpentine channel structure is added at the end of highest branches to increase the convective heat transfer area.

Fig. 7a shows that the flow paths from the inlet to any highest branch in A, B, C, and D zones are the same. However, from the heat transfer point of the view, the convective heat transfer area per heating area in the four zones is different and the position of A, B, C and D zones is not equal because Zone A is much closer to the inlet and has a higher channel density as part of area of Zone A is covered by the inlet plenum. It is this inequality in the heat transfer aspect that results in the different wall temperature distributions in A, B, C and D zones, i.e., temperatures in Zone A are much lower than in other zones. This kind of

temperature non-uniformity can be reduced by redistributing the fluid flow, with more fluid flows to the zones with a higher temperature. The fractal-shaped structure provides the flexibility for doing this. According to fluid mechanics theory, the flow redistribution can be realized by changing the channel geometric size (both of the hydraulic diameter and the length of microchannels) of the branches, consequently, changing the flow resistance characteristics of the channel. Therefore, as shown in Fig. 7b, the channel size of the 3rd branch in Zone A is modified to be smaller than that of other zones in order to reduce the fluid flow rate to Zone A and increase the fluid flow rate to B, C, D zones as the total flow rate is fixed for the whole microchannel network. Under the same principle, in order to allocate more fluid to the high temperature locations within the B, C and D zones, the 2nd branches of B, C and D zones are lengthened compared with that of Zone A as shown in Fig. 7b. The flexibility in the modification of local channel size for the fractal-shaped microchannel provides an easy way to eliminate hotspots in the heat sink for microelectronic cooling.

In summary, the following modifications can be used to improve the performance of a fractal -shaped microchannel network in a heat sink:

(1) Enlarging the channel width of the first four branches (the depth of channel is kept unchanged), in order to reduce the pressure drop and the temperature non-uniformity.
(2) Increasing convective heat transfer area at highest branches by adding serpentine channels at the end of the highest branches, in order to lower the temperature of hotspots and thereby to reduce thermal resistance and temperature non-uniformity.
(3) Changing the local channel width (the depth of channel is kept unchanged) to redistribute more fluid flow to the hotspots.

Although the detailed channel size of the modified fractal-shaped microchannel is not indicated in Fig. 7b, it can readily be calculated since some channel sizes have already been known and the figure is drawn to scale. It can be shown that the convective heat transfer area of the modified fractal-shaped microchannel network is 514 mm^2, almost increased by 150% compared with the convective heat transfer area of 212 mm^2 for the original fractal fractal-shaped microchannel before modifications.

To check the improvement of the modified fractal-shaped microchannel network heat sink, a numerical simulation was conducted under the same mass flow rate and heat flux as the baseline case. The temperature distribution of the bottom wall for the modified fractal shaped microchannel network heat sink is shown in Fig. 8. Comparing with Fig. 6, it can be seen that great improvement in temperature uniformity has been achieved. The numerical results show that the highest temperature of heat sink decreases from 330.9 K to 324.8 K while the lowest temperature of heat sink increases from 318.0 K to 316.3 K, corresponding to a decrease of thermal resistance by 20% and heat sink temperature difference by 34%. As for pressure drop, the total pressure drop of the modified fractal-shaped microchannel network is calculated to be 50.3 kPa, which is about 21% less than the normal fractal-shaped microchannel network. Thus, the modifications not only lead to great improvement in thermal performance, but also lead to smaller pressure drop. This is because the pressure head has been much more properly distributed at different branch levels by the modification of channel size.

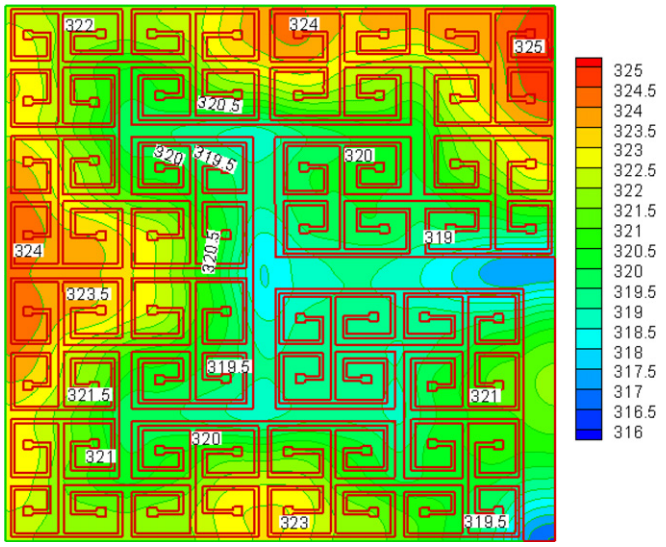

Fig. 8. Temperature distribution at the heating surface for the modified fractal-shaped microchannel heat sink.

8. Comparison with parallel microchannels

A square heat sink with parallel microchannels with the same base dimensions as the fractal-shaped microchannel network heat sink, (i.e., the width of 12 mm, the length of 12 mm and the thickness of 0.5 mm) was also designed. The channel size of parallel microchannels is assumed to be the same with that of the highest branch in the fractal-shaped microchannel (see Table 1), i.e. the width of 0.043 mm and the depth of 0.3 mm. The center-to-center distance between the microchannels is chosen to be 0.1 mm, which was based on the consideration of MEMS fabrication. As a result, the wall thickness of parallel microchannel is 0.057 μm, which is also the thinnest wall thickness in the modified fractal-shaped microchannel heat sink. Under this condition, 120 parallel microchannels with the length of 12 mm can be etched within the heat sink. The numerical model and assumptions of the parallel microchannels heat sink are the same as the fractal-shaped microchannel network heat sink. The inlet and outlet plenum sections of the parallel microchannel heat sink are not included in the computational domain. It can be calculated that the convective heat transfer area of parallel

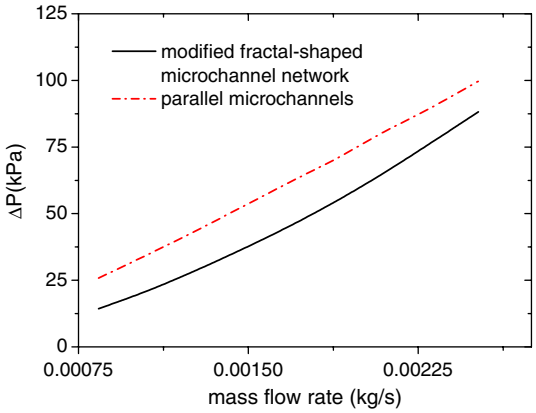

Fig. 9. Variation of pressure drop with mass flow rate for the modified fractal-shaped microchannel network and parallel microchannels.

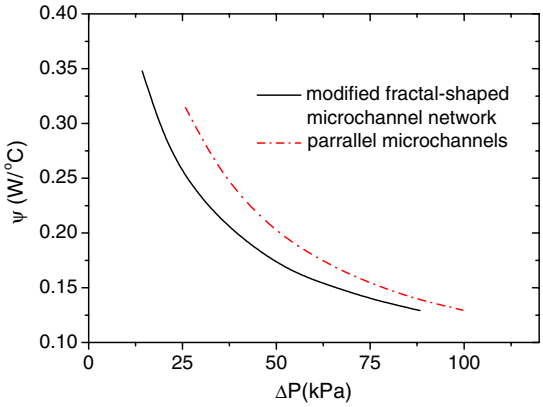

Fig. 10. Variation of thermal resistance with pressure drop for the modified fractal-shaped microchannel network and parallel microchannels.

channels is 925 mm^2, which is much higher than 514 mm^2 of the modified fractal-shaped microchannel network heat sink as indicated earlier in the text.

Fig. 9 shows the variation of pressure drop with the mass flow rate for both parallel microchannels and the modified fractal-shaped microchannel network. It can be seen that for the parallel microchannels, the relationship of the pressure drop with mass flow rate is almost linear, while for the modified fractal-shaped microchannel network, a non-linear relationship is observed. The linear relationship for the case of parallel microchannels agrees well with the classical theory of hydrodynamically fully-developed laminar flow, because the developing segment can be neglected for the parallel microchannels as the ratio of channel length to channel diameter is as large as about 150 in the present case. The reasons for non-linear relationship of pressure drop with mass flow rate for modified fractal-shaped channel network has been explained earlier in the text. Fig. 9 shows although with the additional pressure drop at bifurcations, the total pressure drop of the modified fractal-shaped microchannel network is much smaller than that of the parallel microchannels, indicating that the modified fractal-shaped channel structure is better than parallel channels for the fluid flow distribution. This is especially true when the flow rate is small because the effect of bifurcations on pressure drop is smaller.

Considering the pressure head provided by a micro pump is relatively small and a high pressure drop is not desired for electronic cooling application as mentioned above, it is extremely important to control the pressure drop of the micro heat sink. Therefore, a comparison of the thermal performance of a micro heat sink conducted under the condition of same pressure drop may be more appropriate than that based on the same mass flow rate. Fig. 10 shows the variation of thermal resistance with pressure drop for both parallel microchannel heat sink and the modified fractal-shaped microchannel network heat sink. It is observed that for both heat sinks, the thermal resistance decreases with the increase of pressure drop. The decreasing rate of thermal resistance slows down when pressure drop increases. It is also found that although the convective heat transfer area of the modified fractal-shaped microchannel network heat sink is only about half of the parallel microchannel heat sink, the thermal resistance of the modified fractal-shaped microchannel network heat sink is still lower than that of parallel channels, but the difference decreases when the pressure drop increases. It can be calculated that the thermal resistance of the modified fractal-shaped microchannels is 20.6% and 9.1% less than parallel channels when the pressure drop is 28 kPa and 90 kPa, respectively. This is because when the mass flow rate increases, the pressure drops of fractal-shaped like microchannel network increases faster than that of parallel microchannels as shown in Fig. 9.

Fig. 11 shows the heat sink bottom wall temperature difference as a function of pressure drop. It is revealed that the wall temperature difference of the modified fractal-shaped microchannel network heat sink is much smaller than that of parallel channel heat sink, and the difference decreases with the increase of pressure drop. For example, at pressure drop of 25 kPa and 85 kPa, the temperature dif-

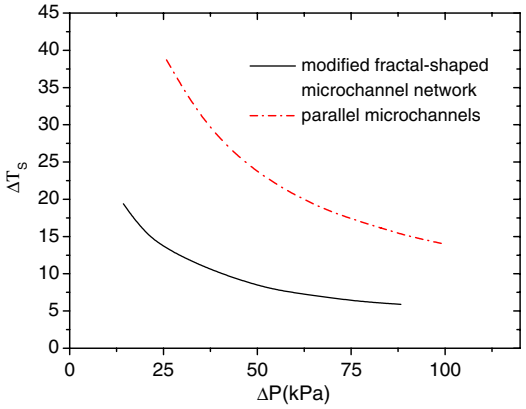

Fig. 11. Variation of temperature difference at the heat sink bottom wall with pressure drop for the modified fractal-shaped microchannel network and parallel microchannels.

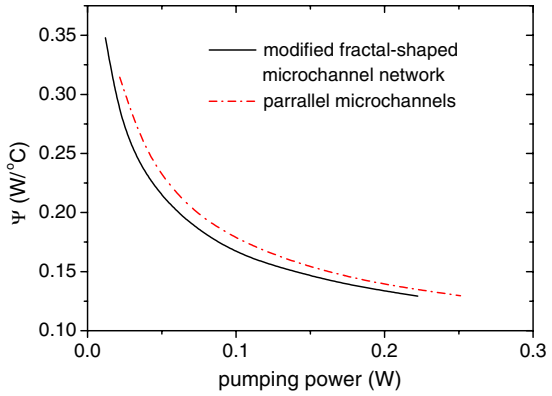

Fig. 12. Variation of thermal resistance with pump power for the modified fractal-shaped microchannel network and parallel microchannels.

ference of the modified fractal-shaped microchannel network heat sink is 13 °C and 7.5 °C, respectively, compared to 45 °C and 22 °C of the parallel microchannel heat sink.

To compare the energy efficiency of a heat sink, the thermal resistance of the modified fractal-shaped microchannel network heat sink and parallel microchannels heat sink is compared under the same pumping power, as shown in Fig. 12. It is observed that the energy efficiency of the modified fractal-shaped microchannel network is also higher.

In summary, the modified fractal-shaped microchannel network heat sink is much better than that of parallel channels heat sink with respect to pressure drop, thermal resistance and temperature uniformity. This advantage is much more obvious when the flow rate or the pressure drop is low, which is favored because high pressure drop is not recommended in practice for the design of microsystems.

9. Conclusions

In this paper, a 3-D numerical simulation, taking into consideration conjugate heat transfer, was conducted to study the hydrodynamic and thermal characteristics of fractal-shaped microchannel for microelectronic cooling application. A comparison of the performance of a modified fractal-shaped microchannel network heat sink with that of a parallel microchannels heat sink is made based on the same heat sink dimensions instead of the same convective heat transfer area as in previous work. The following conclusions can be made from the present study:

(1) The relationship of pressure drop with mass flow rate for the fractal-shaped microchannel network is nonlinear due to the effect of bifurcations and the developing of fluid flow at branches.
(2) The conjugate heat transfer has to be considered in the study of fractal-shaped microchannel network heat sink to predict the thermal characteristics accurately.
(3) The optimization principle of channel network design for fluid flow based on fixed channel volume is not appropriate for the design of heat sinks for microelectronic cooling.
(4) Due to the structural limitation of fractal-shaped microchannel network, hotspots may appear on the bottom wall of the heat sink where the channel density is sparse. The flexible flow distribution of the modified fractal-shaped microchannel network makes it possible to eliminate hotspots in heat sinks by local modifications of the channel size. As a result, the performance of the modified fractal-shaped microchannel network heat sink can be greatly improved.
(5) The modified fractal-shaped microchannel network heat sink has lower thermal resistance, much better temperature uniformity, and much less pressure drop than parallel microchannels heat sink. Therefore, it is promising to be used for microelectronic cooling applications in the future.

Acknowledgements

This work was supported by Intel Company under contract #4507165737 and #4507237867, and partially supported by Shanghai Municipal Science & Technology Committee through Key Fundamental Project No. 05JC14025.

References

[1] J. Darabi, M.M. Ohadi, D. DeVoe, An electrohydrodynamic polarization micropump for electronic cooling, J. Microelectromech. Syst. (10) (2001) 98–106.
[2] A. Bar-Cohen, Optimization of vertical pin-fin heat sinks in natural convective heat transfer, in: Proceedings of 11th International Heat Transfer Conference, Kyonju, Korea, 1998, pp. 501–506.
[3] D.B. Tuckerman, R.F.W. Pease, High performance heat-sinking for VLSI, IEEE Electron Dev. Lett. (2) (1981) 126–129.
[4] X.F. Peng, G.P. Peterson, B.X. Wang, Heat transfer characteristics of water flowing through rectangular microchannels, Exp. Heat Transfer (7) (1994) 265–283.
[5] T.M. Harms, M.J. Kazmierczak, F.M. Gerner, Developing convective heat transfer in deep rectangular microchannels, Int. J. Heat Fluid Flow (210) (1999) 149–157.
[6] Weilin Qu, Gh. Mohiuddin Mala, Dongqing Li, Heat transfer for water flow in trapezoidal silicon microchannels, Int. J. Heat Mass Transfer (43) (2002) 3925–3936.
[7] H.Y. Wu, P. Cheng, An experimental study of convective heat transfer in silicon microchannel with different surface condition, Int. J. Heat Mass Transfer (46) (2003) 2547–2566.
[8] Weilin Qu, Issam Mudawar, Experimental and numerical study of pressure drop and heat transfer in a single-phase micro-channel heat sink, Int. J. Heat Mass Transfer (45) (2002) 2549–2565.
[9] H.Y. Zhang, D. Pinjala, T.N. Wong, K.C. Toh, Y.K. Joshi, Single-phase liquid cooled microchannel heat sink for electronic packages, Appl. Thermal Eng. (25) (2005) 1472–1487.
[10] A. Bejan, Constructal-theory network of conducting paths for cooling a heat generating volume, Int. J. Heat Mass Transfer (40) (1997) 799–810.
[11] A. Bejan, M.R. Errera, Convective trees of fluid channels for volumetric cooling, Int. J. Heat Mass Transfer (43) (2000) 3105–3118.
[12] Deborah V. Pence, Reduced pumping power and wall temperature in microchannel heat sinks with fractal-like branching channel networks, Microscale Thermophys. Eng. (5) (2002) 293–311.
[13] Y. Chen, P. Cheng, Heat transfer and pressure drop in fractal tree-shaped microchannel nets, Int. J. Heat Mass Transfer (45) (2002) 2643–2648.

[14] S.M. Senn, D. Poulikakos, Laminar mixing, heat transfer and pressure drop in tree-shaped microchannel nets and their application for thermal management in polymer electrolyte fuel cells, J. Power Sources (130) (2004) 178–191.
[15] J. Li, G.P. Peterson, P. Cheng, Three-dimensional analysis of heat transfer in a micro-heat sink with single phase flow, Int. J. Heat Mass Transfer (47) (2004) 4215–4231.
[16] A.Y. Alharbi, D.V. Pence, R.N. Cullion, Thermal characteristics of fractal-like microscale branching channels, J. Heat Transfer (126) (2004) 744–752.
[17] C.D. Murray, The physiological principle of minimal work in vascular system, and the cost of blood-volume, Proc. Acad. Natl. Sci. (12) (1926) 207–214.
[18] A. Bejan, M.R. Errera, Deterministic tree networks for fluid flow: geometry for minimal flow resistance between a volume and a point, Fractals (5) (1997) 685–695.
[19] W. Wagner, A. Kruse, Properties of Water and Steam, Springer-Verlag, Berlin Heidelberg, Germany, 1998.
[20] C.J. Glassbrenner, G.A. Slack, Thermal conductivity of silicon and germanium from 3 K to the melting point, Phys. Rev. (134) (1964) A1058–A1069.
[21] A.S. Okhotin, A.S. Pushkarski, V.V. Gorbachev, Thermophysical Properties of Semiconductors, Atom Publ. House, Moscow, 1972.
[22] Y. Nakayama, R.F. Boucher, Introduction to Fluid Mechanics, Butterworth Heinemann, Linacre House, Jordan Hill, Oxford, 2000.